

Experimental Studies of Combustor Dilution Zone Aerodynamics, Part II: Jet Development

S. J. Stevens* and J. F. Carrotte†

University of Technology, Loughborough, England, United Kingdom

Measurements have been made downstream of 16 heated dilution jets injected into a confined annular crossflow in order to investigate inconsistencies in the temperature distribution and the development of individual jets around the annulus. When the dilution air is supplied from a representative feed annulus, the resulting approach velocity produces a complex flowfield that issues through the rear of each dilution hole and, which varies from one jet to another. Measurements of both temperature and velocity in planes parallel and perpendicular to the injection wall have indicated the influence of the exit velocity profiles on the subsequent development of two jets. The structure of a jet is modified by the exit velocity profile, causing distortions of the temperature distribution about the hole center plane. Since each jet has its own mixing characteristics, an irregular temperature pattern around the dilution annulus is produced. Mean vorticity values are calculated from the velocity data and are used to explain differences between the structures of the jets defined here and those of the well-documented single jet issuing into a relatively unconfined crossflow.

Nomenclature

D	= diameter of dilution holes
J	= momentum flux ratio ($= \rho_j V_j^2 / \rho_c V_c^2$)
R_p	= radius of plunging on dilution holes
r	= radius
r_i	= inner radius of crossflow annulus
r_o	= outer radius of crossflow annulus
S	= distance between dilution holes
T	= corrected temperature
T_c	= reference crossflow temperature
T_j	= reference jet temperature
U, V, W	= velocities in X, Y, Z directions
V_c	= velocity of crossflow
V_j	= velocity of jet
X	= coordinate measured from hole center in downstream direction
Y	= coordinate measured normal to injection wall in radial direction
Z	= coordinate measured from hole center in lateral direction
θ	= nondimensional temperature [$= (T - T_c) / (T_j - T_c)$]
ν	= effective kinematic viscosity
$\Omega_x, \Omega_y, \Omega_z$	= vorticity in X, Y, Z directions

Introduction

A JET of fluid injected normally into a crossflow occurs in numerous situations and has therefore led to a large number of theoretical and experimental studies, which have been conducted over many years. This investigation involves a row of jets being injected into a confined crossflow and therefore simulates the mixing processes that occur in the dilution zone of gas turbine combustion chambers. Relatively cold jets of air are injected at the rear of a combustor to dilute the hot

mainstream flow and so are a major factor in ensuring the outlet temperature distribution consistent with the integrity of the downstream turbine stage.

Many workers have undertaken research related to this specific application, and the authors¹ have already reviewed much of this work in the context of the present investigation. Nearly all of the published data, however, has concentrated on the mean radial temperature profile, but of equal importance is the consistency of the temperature pattern around the annulus. The avoidance of local "hotspots" or circumferential irregularities in the outlet temperature distribution is particularly important since this can have serious consequences in terms of engine performance and durability of the nozzle guide vanes and turbine blades. Even in experiments with carefully controlled primary zone exit distributions such irregularities do occur, often in a random manner, and vary in magnitude and position with different combustors built to the same design. As was found by Moys and Stevens,² it is only when the combustor casing is removed and the dilution air supplied from an unrepresentative plenum chamber are the temperature irregularities removed. One possible source of such irregularities is variations in the behavior of the dilution jets, and this experimental program has therefore been concerned with the consistency of the temperature pattern downstream of a row of jets injected into a confined crossflow.

Review of Previous Work at Loughborough

A major influence on jet behavior is the way air is supplied to the dilution holes, and previously published work¹ has described and quantified the irregularities observed in the behavior of dilution jets when air is supplied from a representative feed annulus. The temperature distribution two diameters downstream of three adjacent holes (Fig. 1) illustrates the differing degrees of distortion or apparent "twisting" of each jet about its centerplane which is responsible for the irregular temperature pattern in the annulus of the dilution zone.

The importance of the feed conditions to the dilution holes makes it necessary to simulate the annulus formed by the combustor liner and outer casing so that the approach flow direction is approximately perpendicular to the axial centerline of each hole. The deflection of the flow as it passes from the feed annulus through the dilution hole has a major influence on the velocity profile across the exit plane, producing an extremely complex flowfield in the ensuing jet that varies in a random manner from one jet to another (Fig. 2). This paper is a continuation of the previous work and analyzes the initial

Presented as Paper 88-3274 at the AIAA/ASME/SAE/ASCE 24th Joint Propulsion Conference, Boston, MA, July 11-13, 1988; received Sept. 23, 1988; revision received Feb. 15, 1989. Copyright © 1988 by the American Institute of Aeronautics and Astronautics, Inc. All rights reserved.

*Professor of Aeronautical Propulsion, Department of Transport Technology.

†Research Assistant, Department of Transport Technology.

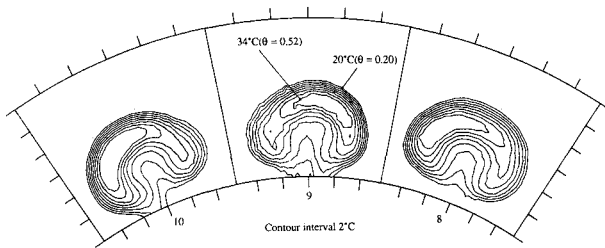


Fig. 1 Temperature distribution for holes 8 to 10 ($X/D = 2.0$).

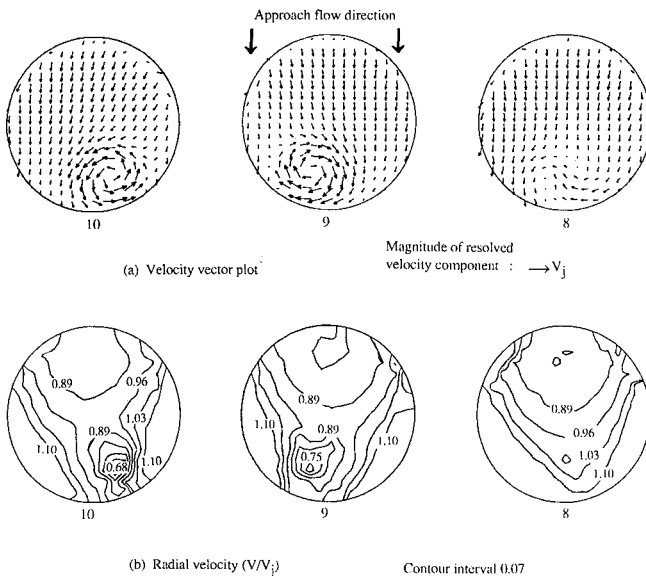


Fig. 2 Velocity distributions across the exit planes of holes 8-10 ($Y/D = 0.05$).

development of two dilution jets close to the injection plane, indicating how the complex flowfield located in the rear of each jet influences its mixing characteristics. The two jets selected were those issuing from holes 8 and 10, which exhibit similar degrees of distortion in their temperature distribution at $X/D = 2.0$ but which have different velocity profiles across their exit planes.

The investigation was conducted on the same fully annular test facility and at the same operating conditions at which the previously published data were obtained. All dilution measurements were performed at a jet-to-crossflow momentum flux ratio of 4, with an approach velocity in the feed annulus of approximately 7 m/s and a mean jet velocity V_j of 29.5 m/s.

Characteristics of Jets in a Crossflow

The nature of this research program makes it necessary to analyze the structure of individual dilution jets and relate this to the downstream flowfield and the observed irregularities in the temperature distribution. As will be shown, there are significant differences between the results presented here and those relating to the well-documented studies of a single jet issuing into a relatively unconfined crossflow. However, as outlined by Moussa et al.,³ the geometrical configuration surrounding a jet as it issues into the crossflow plays a crucial role in determining the subsequent mixing and development processes.

As each jet of fluid issues from a dilution hole it creates a blockage in the crossflow, and as a consequence the flow immediately ahead of the jet decelerates, causing an increase in pressure. Downstream a rarefaction occurs and this, combined with the increased upstream pressure, provides a force that deforms the jet. Intensive mixing between the crossflow and jet fluid results in the rapid development of a turbulent

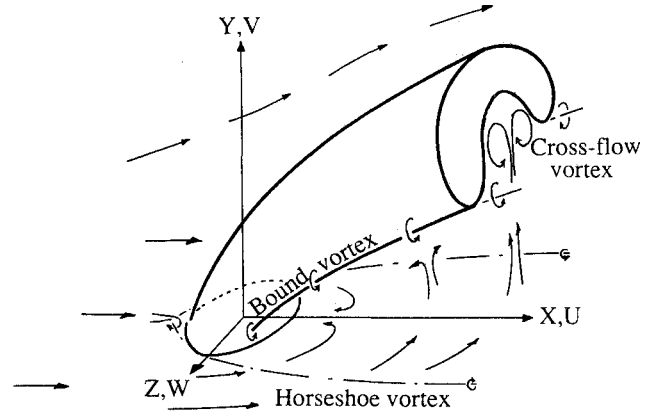


Fig. 3 Multiple jets in a crossflow.

shear layer around the periphery of the jet, and the more curved trajectory of this lower momentum fluid at the sides of the jet contributes to the development of the characteristic "kidney"-shaped jet profile. Downstream of the injection plane the flowfield is dominated by several vortex systems (Fig. 3), and it is these that mainly control the entrainment and mixing of the crossflow and jet fluid.

A horseshoe vortex system is formed by the oncoming vorticity associated with the boundary layer on the injection wall being deflected around the jet, a feature, which is analogous to when flow is deflected around a cylinder mounted on a flat surface. Streamwise (Ω_x) vorticity is thereby formed that is negative on the positive side of the Z axis, but its effect on fluid mixing is relatively small in comparison with two other regions of high vorticity.

As outlined by Andreopoulos and Rodi,⁴ vorticity is generated at the interface of the initially orthogonal jet and crossflow in addition to the components of vorticity in the jet issuing from the dilution hole. Streamwise (Ω_x) vorticity is generated by the high radial velocity gradients ($\partial V/\partial Z$) at the sides of the jet, the fluid rolling up to form a pair of bound vortices that are much stronger and are of opposite vorticity than the aforementioned horseshoe vortex system. The bound vortices are located at the lobes of each jet and therefore enhance the kidney-shaped profile of the jet as it progresses downstream.

In the case of multiple jets issuing into a confined crossflow, two further vortices are formed by crossflow fluid that passes between the jets and into the low pressure wake region. Close to the wall the fluid moves in a predominantly lateral direction with very little axial momentum, the inward fluid movement being assisted by the bound vortex system. This fluid becomes entrained by the jet and rolls up to form two crossflow vortices in the jet wake.

Superimposed on the described flow structure is the effect of the velocity profile across the exit plane of the dilution hole. The complex flowfield that issues through the rear of the hole modifies the mechanisms by which the crossflow is entrained and mixed with the jet fluid.

Test Facility

The test facility (Fig. 4) is comprised of three vertically mounted concentric Plexiglas tubes that form a dilution hole feed annulus of 35.8-mm height and a crossflow annulus of 76.2-mm height. The array of dilution jets is formed by 16 equispaced 25.4-mm-diam plunged holes ($R_p/D = 0.375$) located in the center casing and set at a spacing/hole diameter ratio of 2.75. A detailed description of the test facility, instrumentation, and data processing is given in previously published work.¹

Air prior to entering the dilution hole feed annulus is passed through a heater, so raising its temperature above that of the crossflow. Supplying heat in this way gives information on the

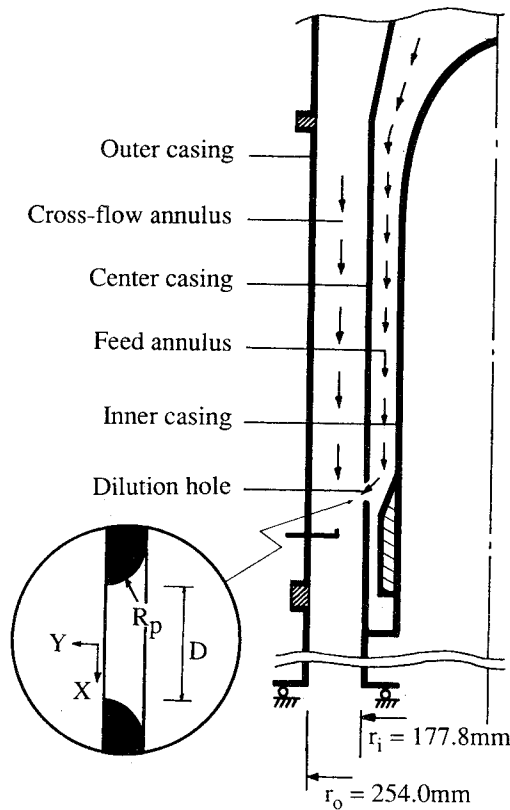


Fig. 4 Test facility.

mixing of the jet fluid as well as identifying the trajectory of the high-temperature core. Chromel/Alumel thermocouples connected to Comark digital thermometers record temperatures both in the dilution zone and upstream of the injection plane in both the crossflow and feed annuli. Results are presented as contours of corrected temperature for reference conditions of $T_j = 55^\circ\text{C}$ and $T_c = 11^\circ\text{C}$.

Flow angles and velocities were measured with five-hole pressure probes, overall diameter 1.73 mm, and were used in the nonnull mode using the calibration procedure outlined by Wray.⁵ All pressure readings were corrected to a reference jet dynamic head of 50-mm water gauge, and the data derived from the five-hole probe measurements are presented in terms of velocity distributions. Resolved components of velocity in the traversing plane are presented in the form of vectors, though streamlines should not be inferred from the arrows since the flowfield is strongly three-dimensional, particularly close to the injection plane. Contours of constant velocity are used to indicate the magnitude of the velocity components perpendicular to the traverse plane and, like the vector arrows, are nondimensionalized by the mean jet velocity (V_j). Despite the use of several probes with different geometries, there are regions of the flowfield that remain outside the probe calibration ranges of ± 35 deg in pitch and yaw. Data points are omitted in these regions, although in certain areas where only one flow angle is outside the calibration limits, an indication of the flow direction in one plane may be given, and where this has been done the data are represented by a dotted line.

All of the data presented are based on measurements time-averaged over a period of 5 s prior to being committed to the memory of a DEC LSI 11/23 microcomputer. Measurements in planes perpendicular to the center casing were conducted at $X/D = 0.0, 0.30, 0.54$, and 0.72 for holes 8 and 10, the data being collected at nominal lateral (Z) and radial (Y) spacings of $0.06D$ and $0.1D$, respectively. Data recorded in several planes parallel to the center casing was done so at a nominal spacing of $0.06D$ in both the lateral (Z) and streamwise (X) directions.

Parameter Definitions

The measured temperatures are corrected using the non-dimensional parameter θ where

$$\theta = \frac{T - T_c}{T_j - T_c} \quad (1)$$

Because of the large injection wall radius, vorticity is calculated using formulas based on a Cartesian coordinate system so that

Streamwise vorticity:

$$\Omega_x = \frac{\partial W}{\partial Y} - \frac{\partial V}{\partial Z} \quad (2)$$

Radial vorticity:

$$\Omega_y = \frac{\partial U}{\partial Z} - \frac{\partial W}{\partial X} \quad (3)$$

where each gradient is evaluated from the mean velocity data to which is fitted a three-term Lagrange polynomial in the region of interest. Results are presented in terms of vorticity contours that are nondimensionalized using the mean jet velocity V_j and the dilution hole diameter D .

The equations for the rate of change of vorticity can be derived from the Navier-Stokes equations so that for the x component

$$\begin{aligned} \frac{\partial \Omega_x}{\partial t} + U \frac{\partial \Omega_x}{\partial X} + V \frac{\partial \Omega_x}{\partial Y} + W \frac{\partial \Omega_x}{\partial Z} = \Omega_x \frac{\partial U}{\partial X} + \Omega_y \frac{\partial U}{\partial Y} \\ + \Omega_z \frac{\partial U}{\partial Z} + \nu \left(\frac{\partial^2 \Omega_x}{\partial X^2} + \frac{\partial^2 \Omega_x}{\partial Y^2} + \frac{\partial^2 \Omega_x}{\partial Z^2} \right) \end{aligned}$$

or substantial derivative form

$$\begin{aligned} \frac{D\Omega_x}{Dt} = \left(\Omega_x \frac{\partial U}{\partial X} + \Omega_y \frac{\partial U}{\partial Y} + \Omega_z \frac{\partial U}{\partial Z} \right) \\ + \nu \left(\frac{\partial^2 \Omega_x}{\partial X^2} + \frac{\partial^2 \Omega_x}{\partial Y^2} + \frac{\partial^2 \Omega_x}{\partial Z^2} \right) \quad (4) \end{aligned}$$

The first term on the right side of Eq. (4) represents the production of vorticity due to stretching of the vortex lines, and the second term indicates the diffusion of vorticity due to viscous effects.

Results and Discussion

Initial Development—Hole 8

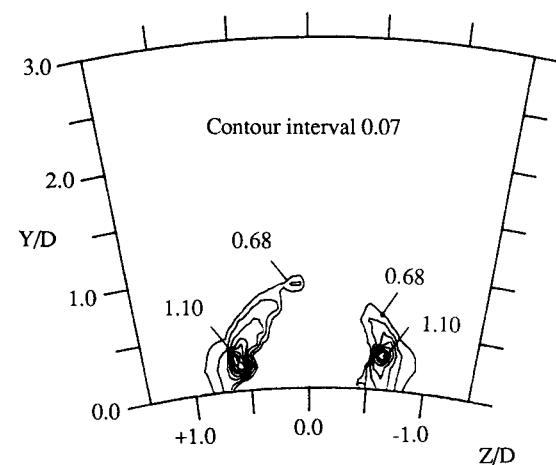
Measurements conducted in planes perpendicular to the downstream (X) direction indicate the initial development of the jet as it issues into the crossflow. The data collected at $X/D = 0.30$ (Fig. 5) illustrate the formation of the bound vortices at the lateral edges of the jet and their influence on the temperature distribution in this region. The velocity data at $X/D = 0.54$ (Fig. 6) show the continued development of these vortices as the jet progresses downstream, but even at this early stage, distortion of the temperature distribution is apparent both in the hot core region of the jet and close to the injection wall.

Measurements conducted parallel to the injection wall indicate the influence of the velocity profile, across the exit plane of the dilution hole, on the subsequent development of the jet and its downstream temperature distribution. The development of the complex flowfield associated with the feed conditions to the dilution holes is evident in the velocity vector plot at $Y/D = 0.2$ (Fig. 7), which also illustrates the internal movement of fluid within the jet. Fluid in the front half of the jet that has been deflected by the crossflow is forced to move around the relatively undeflected flow in the rear of the jet,

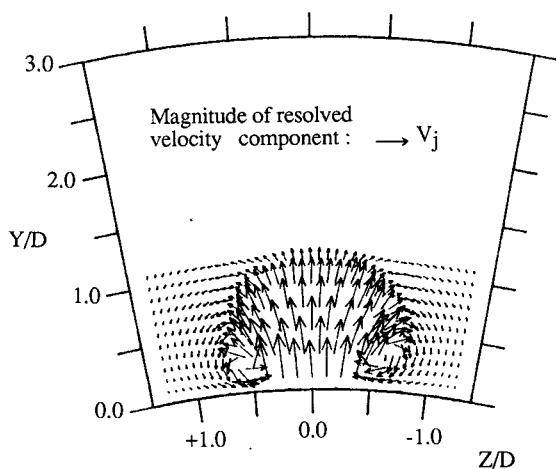
this curvature being indicated by the increase in downstream U velocity components. However, because of the behavior of the fluid issuing through the rear of the dilution hole this deflection is not symmetric about the hole centerplane. Fluid issuing through the positive ($Z > 0$) side of the hole is deflected much more rapidly than fluid on the opposite ($Z < 0$) side of the centerplane, which has to pass over and yaw around the greater effective blockage associated with the complex flow-field. Immediately downstream of the injection plane at $X/D = 0.54$ the velocity profiles at $Z/D = \pm 0.25$ confirm this

observation (Fig. 8), with fluid on the right ($Z < 0$) side of the jet exhibiting greater yawing and penetration into the cross-flow annulus. It is these variations in trajectory, which also affect the jet-path length to a given downstream (X) location, that are responsible for producing the distortion of the core of the jet.

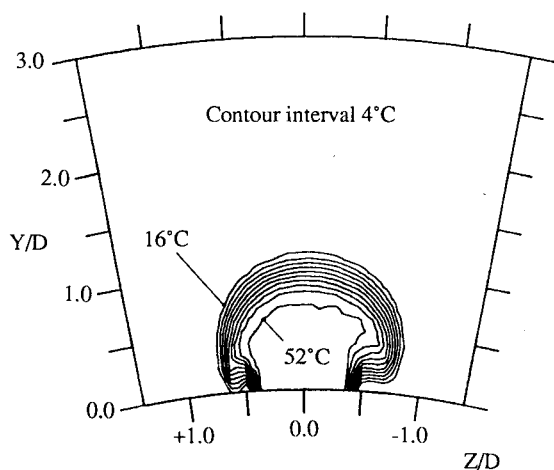
The development of the bound vortices at the lateral edges of the jet must also be influenced by the trajectory of the jet fluid, and this is evident in the temperature distribution at $X/D = 0.30$ (Fig. 5c). Under normal circumstances the vor-



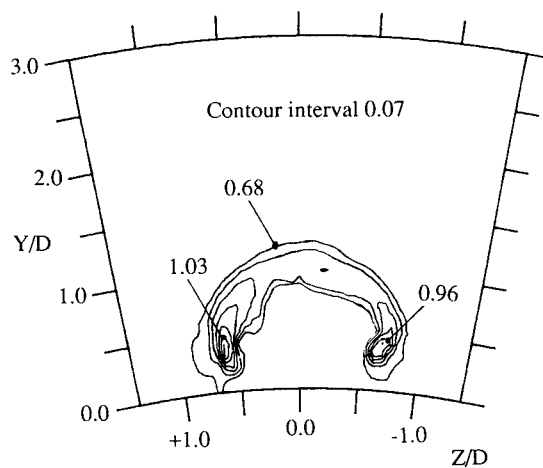
a) Axial velocity distribution (U/V_j)



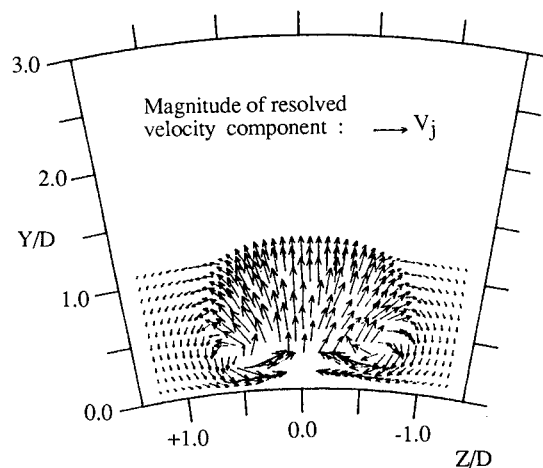
b) Velocity vector plot



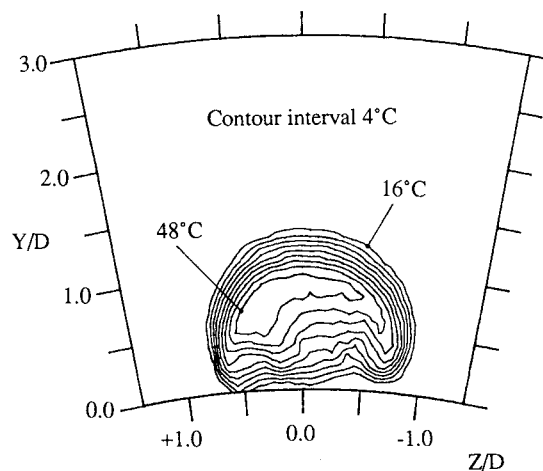
c) Temperature distribution



a) Axial velocity distribution (U/V_j)



b) Velocity vector plot



c) Temperature distribution

Fig. 5 Velocity and temperature distribution (hole 8, $X/D = 0.30$).

Fig. 6 Velocity and temperature distribution (hole 8, $X/D = 0.54$).

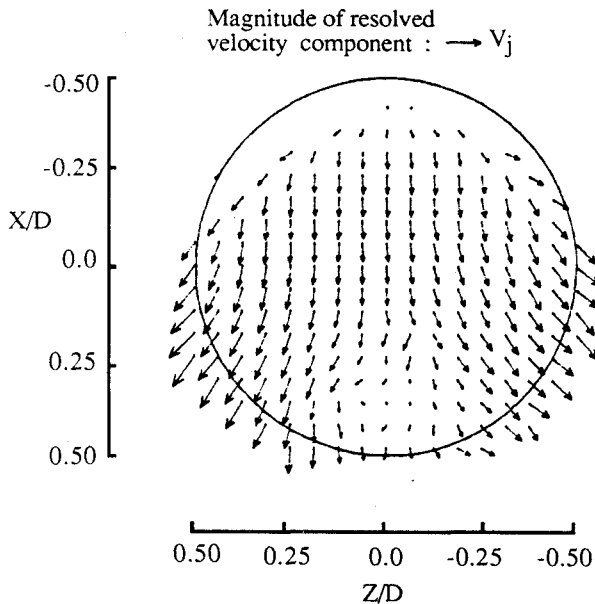


Fig. 7 Velocity vector plot (hole 8, $Y/D = 0.2$).

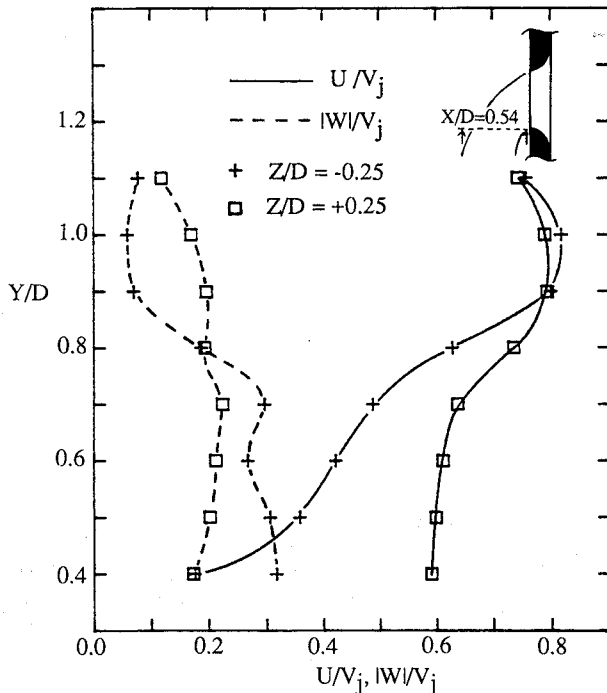


Fig. 8 Streamwise and lateral velocity profiles (hole 8, $X/D = 0.54$).

tices act as a transport mechanism, displacing relatively hot fluid to a lower radius and mixing it with the crossflow. The additional yaw component imparted to one side of the jet increases the lateral spreading of the hot fluid and affects the characteristics of the vortex, as indicated by both the velocity and temperature data at $X/D = 0.30$ (Fig. 5). Since mixing close to the injection wall is controlled by this bound vortex flowfield the different vortex and hence mixing characteristics on either side of the jet are responsible for producing the asymmetry of the temperature distribution at $Y/D = 0.2$ (Fig. 9).

The trajectory of the jet fluid and the different bound vortex mixing characteristics not only directly affect the temperature distribution but also result in different amounts of fluid being supplied from either side of the jet into the wake region. This fluid then rolls up to form the two crossflow

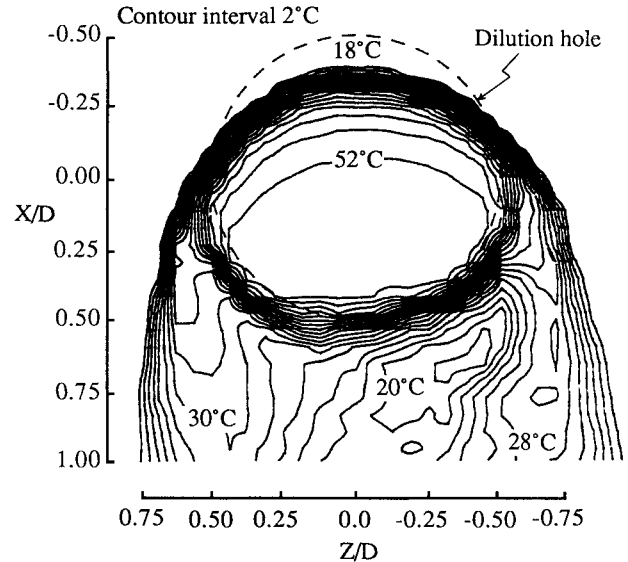


Fig. 9 Temperature distribution (hole 8, $Y/D = 0.2$).

vortices, thus explaining the differences in the size of these flow features that have been recorded at $X/D = 2.0$ (Fig. 10), the temperature distribution at this location having already been presented (Fig. 1). The stronger crossflow vortex will entrain more jet fluid, so producing a recirculating region that transports hot fluid toward the injection wall, thereby ensuring continued distortion of the temperature distribution as the jet progresses downstream.

Initial Jet Development—Hole 10

The approach velocity in the feed annulus produces a well-defined vortex that issues through the rear of hole 10 and is still present at $Y/D = 0.2$ (Fig. 11). Because of its strength and location a large blockage is created, causing a redistribution of fluid about the hole centerplane so that the core of the jet becomes displaced to one side, as illustrated by the temperature distribution at $X/D = 0.54$ (Fig. 12). This redistribution of fluid is also indicated by the axial velocity contours at $X/D = 2.0$ (Fig. 13), which shows a significant difference from that of hole 8 (Fig. 10a) and is therefore the main cause of the temperature distortion recorded in the jet as it progresses downstream. Of secondary importance is the influence of the fluid trajectory on the bound vortex system, the different mixing and decay characteristics on either side of the centerplane producing further distortion of the temperature distribution.

Vorticity Characteristics

There are significant variations between the well-documented structure of a single jet issuing into a relatively unconfined crossflow and the data presented here relating to a multiple-jet configuration. This can be explained when considering the vorticity characteristics of the flow and how they are affected by the velocity field that surrounds each jet as it issues into the confined crossflow.

Bound Vortex System

At the injection plane vorticity is generated by the high radial velocity gradients ($\partial V/\partial Z$ and $\partial V/\partial X$) around the periphery of the jet, which are convected into the streamwise direction. In the multiple-jet configuration the blockage caused by the row of jets in the dilution annulus leads to an acceleration of the crossflow between each jet. Thus, streamwise vorticity (Ω_x) is intensified by the extensional strain rate ($\partial U/\partial X > 0$), producing the well-defined vortices that have been seen in the velocity vector plots at $X/D = 0.30$, and

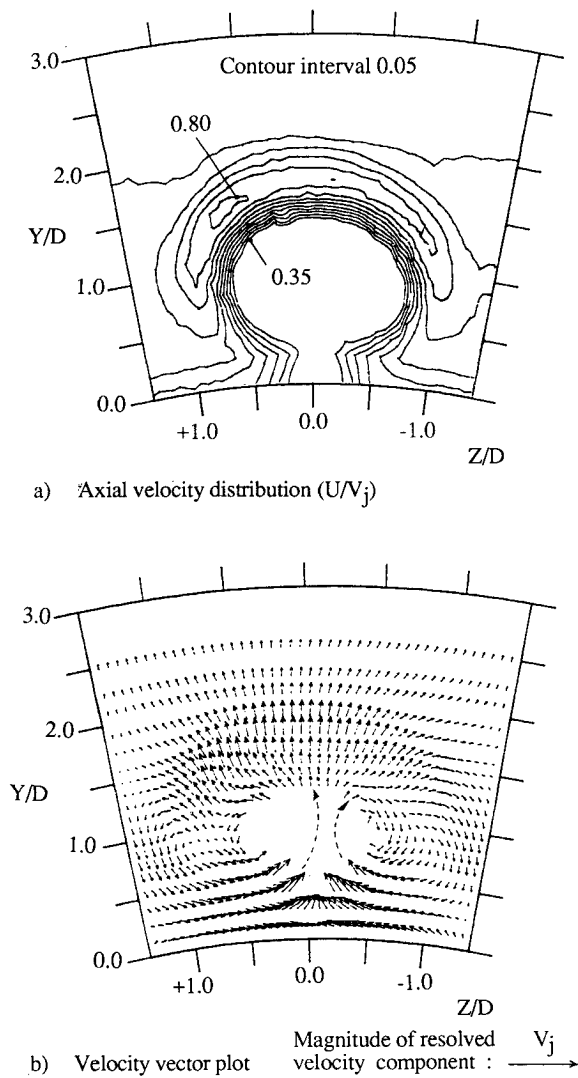


Fig. 10 Velocity distribution (hole 8, $X/D = 2.0$).

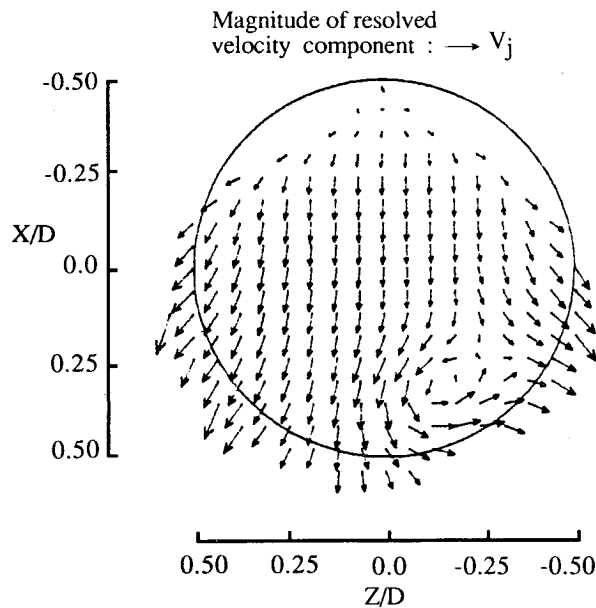


Fig. 11 Velocity vector plot (hole 10, $Y/D = 0.20$).

which is also indicated by the vorticity contours at this same location (Fig. 14). In comparison with a single jet the magnitude of the bound vorticity is much higher but is concentrated in a smaller area. The vorticity contours at $X/D = 0.30$ also appear to indicate the presence of the less-pronounced counter-rotating horseshoe vortex system positioned close to the injection wall. Downstream of the injection plane, crossflow is drawn into the wake region behind each jet so that mass continuity dictates a decrease in the axial velocity component.

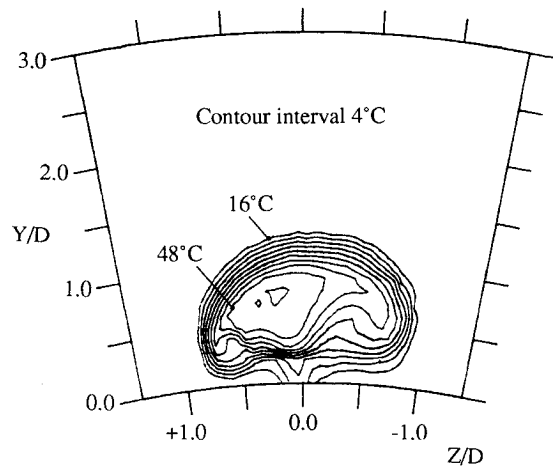


Fig. 12 Temperature distribution (hole 10, $X/D = 0.54$).

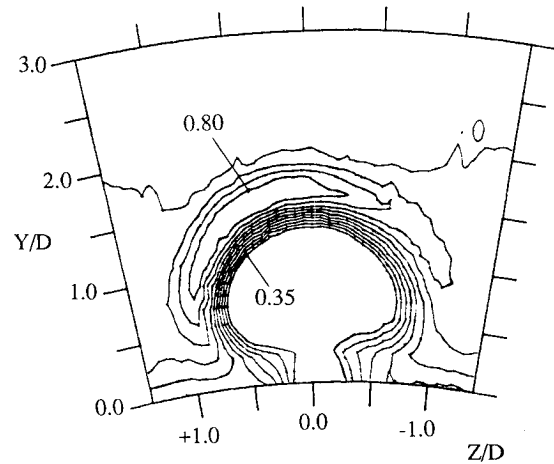


Fig. 13 Axial velocity distribution (U/V_j) (hole 10, $X/D = 2.0$).

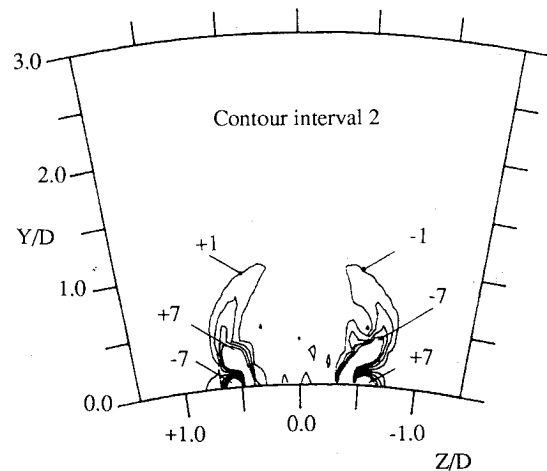


Fig. 14 Streamwise vorticity distribution ($\Omega_x D/V_j$) (hole 8, $X/D = 0.30$).

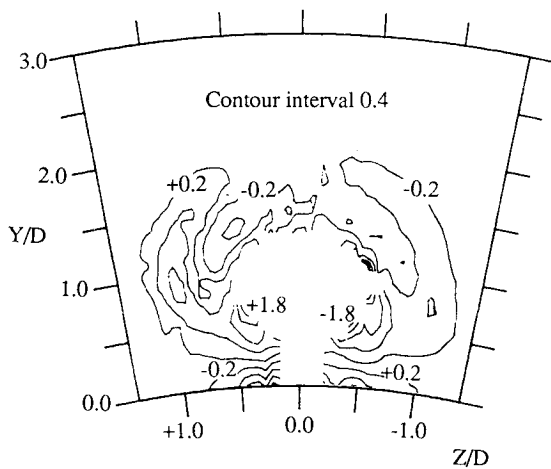


Fig. 15 Streamwise vorticity distribution ($\Omega_x D / V_j$) (hole 8, $X/D = 2.0$).

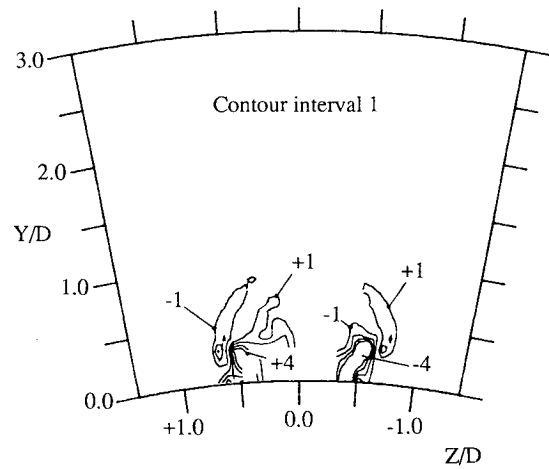


Fig. 16 Radial vorticity distribution ($\Omega_y D / V_j$) (hole 8, $X/D = 0.30$).

Hence, the compressional strain rate ($\partial U / \partial X < 0$) results in a decrease in streamwise vorticity, the magnitude of which can be estimated from the mean velocity data. For example, the axial velocity components at the center of the bound vortex on the left side ($Z > 0$) of hole 8 are 35 and 22 m/s at $X/D = 0.30$ and 2.0, respectively. Using the substantial derivative form of Eq. (4) and assuming a mean axial velocity of 28.5 m/s between these locations, there is an approximately a 45% reduction in streamwise vorticity purely due to the compressional strain rate in the flowfield at the center of the bound vortex. This is the main reason for the rapid decay of the bound vortex system in the multiple-jet configuration and has important consequences when considering the design of the dilution annulus. By maintaining axial velocities in the downstream flowfield the negative vorticity production can be minimized, enhancing mixing, and this explains the findings of Holdeman et al.⁶ concerning the favorable effects of introducing mixing duct convergence.

Of equal importance in terms of vortex decay is the diffusion of vorticity present in both single- and multiple-jet configurations, although the dissipation is enhanced by the greater velocity gradients in the latter case. Since the compressive strain rate is approximately the same on either side of the centerplane, the asymmetry in the bound vortex system at $X/D = 2.0$ (Fig. 15) is mainly due to differences in the diffusion of vorticity associated with variations in the trajectory of jet fluid. As vorticity reflects gradients in momentum that are eroded by turbulent stresses, Reynolds' analogy⁷ suggests that a greater rate of diffusion reflects higher mixing, producing the more rapid rate of cooling that has been observed on the right ($Z < 0$) of the hole 8 centerplane.

Crossflow Vortex System

Measurements conducted at $X/D = 2.0$ indicate the complex nature of the flowfield in comparison with that of the relatively simple bound vortices observed downstream of a single jet. In this case the bound vortex system has almost decayed and although data are limited due to the finite probe calibration range, there does appear to be a large concentration of streamwise vorticity located in the wake of the jet.

Radial components of vorticity must be generated by the lateral shearing between the jet and the crossflow (Fig. 16) and the movement of flow into the separated wake region behind the jet, these effects being enhanced by the surrounding velocity field in a multiple-jet configuration. As outlined by Sykes et al.,⁸ diffusion at the sides of the jet reduces this vorticity component, and behind the jet, viscous effects are relatively small and the component is increased because of an exten-

sional strain rate as fluid in the wake is entrained upward with the jet. This vorticity is convected into the axial direction and is thought to be responsible for the high regions of vorticity observed in the wake at $X/D = 2.0$.

Conclusions

An experimental investigation has been conducted into the structure of multiple jets issuing into a confined crossflow and how this relates to the observed irregularities in the temperature distribution downstream of the injection plane. The following conclusions have been drawn:

- 1) The direction of the approach flow in the feed annulus and its deflection as it passes through the dilution holes produces a complex flowfield in the rear of each jet as it issues into the crossflow.
- 2) This flowfield affects the trajectory of the fluid as the jet develops in the crossflow and is the major factor in producing distortion of the temperature distribution about each hole centerplane.
- 3) In certain cases the velocity profile across the exit plane of a dilution hole can lead to a redistribution of jet fluid about the hole centerplane.
- 4) The fluid trajectory also affects the vortices that develop at the lateral edges of each jet and that control the mixing of fluid in the jet wake.
- 5) Since the complex flowfield varies in a random manner from one jet to another so each jet has its own mixing characteristics, thereby leading to overall irregularity of the temperature pattern in the dilution annulus.
- 6) There are significant differences between the structure of a single-jet issuing into a relatively unconfined crossflow and that of a multiple-jet configuration issuing into a confined crossflow.

Investigations are now being conducted into what changes are necessary to the injection plane geometry so as to yield the subsequent development of a jet insensitive to the effects of the approach velocity in the feed annulus. Controlling jet development in this way should produce a substantial reduction in the temperature irregularities observed at the combustor exit.

Acknowledgments

This work was supported by The Ministry of Defence, Royal Aircraft Establishment, Pyestock, Farnborough, United Kingdom, Contract D/ER1/9/4/2170/113/RAE. The authors also wish to express their appreciation to G. Hodson, R. Marson, and D. Glover for their assistance in the design and construction of the test rig.

References

¹Carotte, J. F., and Stevens, S. J., "The Influence of Dilution Hole Aerodynamics on the Temperature Distribution in a Combustor Dilution Zone," AIAA Paper 87-1827, 1987; see also "Experimental Studies of Combustor Dilution Zone Aerodynamics Part I: Mean flow fields," *Journal of Propulsion and Power*, Vol. 6, No. 3, 1990, pp. 297-304.

²Moys, R. H., and Stevens, S. J., "Asymmetric Jets in an Annulus," Dept. of Transport Technology, Loughborough University, Loughborough, England, United Kingdom, TT83R02, 1983.

³Moussa, Z. M., Trischka, J. W., and Eskinazi, S., "The Near Field in the Mixing of a Round Jet with a Cross-stream," *Journal of Fluid Mechanics*, Vol. 80, 1977, pp. 49-80.

⁴Andreopoulos, J., and Rodi, W., "Experimental Investigation of

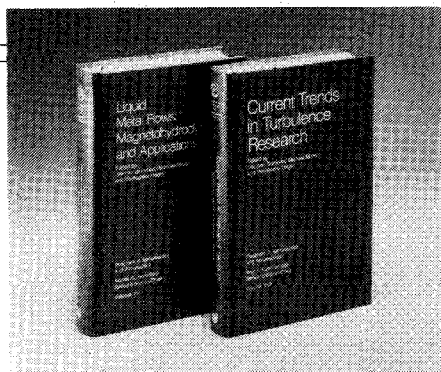
Jets in a Crossflow," *Journal of Fluid Mechanics*, Vol. 138, 1984, pp. 93-127.

⁵Wray, A. P., "The Use of a 5-hole Probe as a Non-nulled Instrument and the Analysis of Test Data Using the Computer Programs 5HP1, 5HP2 and 5HP3," Dept. of Transport Technology, Loughborough University, Loughborough, England, United Kingdom, TT86R02, Jan. 1986.

⁶Holdeman, J. D., Srinivasan, R., and Berenfeld, A., "Experiments in Dilution Jet Mixing," *AIAA Journal*, Vol. 22, No. 10, Oct. 1984, pp. 1436-1443.

⁷Schlichting, H., *Boundary Layer Theory*, McGraw-Hill, New York, 1951.

⁸Sykes, R. I., Lewellen, W. S., and Parker, S. F., "On the Vorticity Dynamics of a Turbulent Jet in a Crossflow," *Journal of Fluid Mechanics*, Vol. 168, 1986, pp. 393-413.



Liquid Metal Flows: Magnetohydrodynamics and Applications and Current Trends in Turbulence Research

Herman Branover, Michael Mond,
and Yeshajahu Unger, editors

Liquid Metal Flows: Magnetohydrodynamics and Applications (V-111) presents worldwide trends in contemporary liquid-metal MHD research. It provides testimony to the substantial progress achieved in both the theory of MHD flows and practical applications of liquid-metal magnetohydrodynamics. It documents research on MHD flow phenomena, metallurgical applications, and MHD power generation. *Current Trends in Turbulence Research (V-112)* covers modern trends in both experimental and theoretical turbulence research. It gives a concise and comprehensive picture of the present status and results of this research.

To Order, Write, Phone, or FAX:



c/o TASC0, 9 Jay Gould Ct., P.O. Box 753
Waldorf, MD 20604 Phone (301) 645-5643
Dept. 415 ■ FAX (301) 843-0159

V-111 1988 626 pp. Hardback
ISBN 0-930403-43-6
AIAA Members \$49.95
Nonmembers \$79.95

V-112 1988 467 pp. Hardback
ISBN 0-930403-44-4
AIAA Members \$44.95
Nonmembers \$72.95

Postage and handling \$4.75 for 1-4 books (call for rates for higher quantities). Sales tax: CA residents add 7%, DC residents add 6%. Orders under \$50 must be prepaid. Foreign orders must be prepaid. Please allow 4 weeks for delivery. Prices are subject to change without notice.